

High-Energy Astrophysics and Cosmology

John Ellis^{a*}

^aTheory Division, CERN,
CH 1211 Geneva 23, Switzerland

Interfaces between high-energy physics, astrophysics and cosmology are reviewed, with particular emphasis on the important roles played by high-energy cosmic-ray physics. These include the understanding of atmospheric neutrinos, the search for massive cold dark matter particles and possible tests of models of quantum gravity. In return, experiments at the LHC may be useful for refining models of ultra-high-energy cosmic rays, and thereby contributing indirectly to understanding their origin. Only future experiments will be able to tell whether these are due to some bottom-up astrophysical mechanism or some top-down cosmological mechanism.

CERN-TH/2002-300

astro-ph/0210580

1. Introduction

There are two ways in which high-energy particles have appeared naturally in the Universe: one is via energetic astrophysical sources such as gamma-ray bursters (GRBs) or active galactic nuclei (AGNs), and the other is via the characteristically high particle energies in the very early Universe. In this talk, I illustrate the possible rôles of both these types of sources, and discuss some related open questions in relation to the cosmic-ray energy spectrum shown in Fig. 1. Here are a few examples.

Even relatively ‘low-energy’ parts of this spectrum in the range $1 \sim 10$ GeV are directly connected to ultra-high-energy particle physics, via their rôle in producing atmospheric neutrinos [2], one of our windows on Grand Unified Theories (GUTs). Somewhat higher-energy parts of the spectrum up to energies ~ 1 TeV are relevant to the experimental search for cold dark matter particles. Confirmed observations of GRBs have been limited to the MeV energy range, but there are unconfirmed reports of observations in the GeV and even TeV [3] energy ranges, and GRBs might even be responsible for the ultra-high-energy cosmic rays (UHECRs). Alternatively, these might be due to some exotic top-down mechanism involving the de-

cays of supermassive particles produced in the very early Universe [4], or some other extreme astrophysical sources. Either way, they may provide a unique laboratory to look for violations of fundamental principles such as Lorentz invariance [5].

Before discussing these possible playgrounds for high-energy physics, let us first review the basis for the Big-Bang cosmology that plays an essential rôle in the following sections of this talk.

2. Big-Bang Cosmology

According to standard Big-Bang cosmology, the entire visible Universe is expanding homogeneously and isotropically from a very dense and hot initial state. Apart from the present Hubble expansion, the first piece of evidence for the Big Bang was the cosmic microwave background (CMB) radiation, which is thought to have been emitted when the Universe was about 3000 times smaller and hotter than it is today, with age $\sim 3 \times 10^5$ y. The CMB has a dipole deviation from isotropy at the 10^{-3} level, which this is believed to be due to the Earth’s motion relative to a Machian cosmological frame.

The second piece of evidence for the Big Bang was provided by the abundances of light elements seen in Fig. 2, which are thought to have been established when the Universe was about 10^8 times smaller and hotter than it is today, with age ~ 1 to 10^2 s. This nuclear

*Talk presented at the XIIth International Symposium on Very-High-Energy Cosmic-Ray Interactions, CERN, July 2002

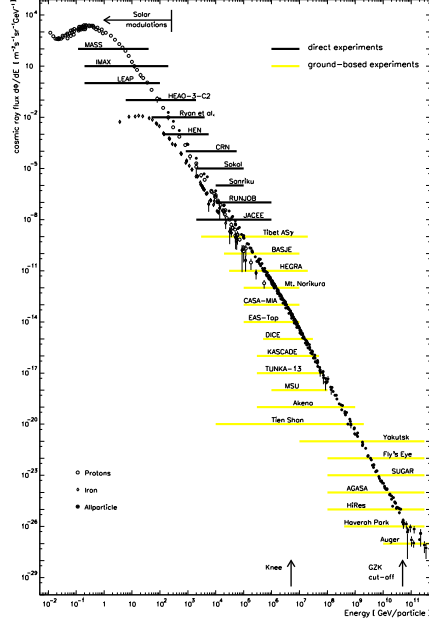


Figure 1. The cosmic-ray spectrum extends over many decades in energy, which are sampled by many different experiments [1].

‘cooking’ must have occurred when the temperature T of the Universe corresponded to characteristic particle energies ~ 1 MeV.

Before this time, when it was $\sim 10^{-6}$ to $\sim 10^{-5}$ s old, it is thought that the Universe made a transition from quarks and gluons to hadrons at a temperature $T \sim 100$ MeV. Previous to that, the electroweak transition when Standard Model particles acquired their masses would have occurred when the Universe was $\sim 10^{-12}$ to $\sim 10^{-10}$ s old, and the temperature $T \sim 100$ GeV. The CMB is thought to provide a window to an even earlier epoch, via its small-scale fluctuations $\delta\rho/\rho$, which show up at the 10^{-5} level, as seen in Fig. 3. If these are due to quantum fluctuations during an inflationary epoch, $\delta\rho/\rho \sim (T/m_P)^2$, telling us that the typical energies of particles in the Universe may once have approached 10^{16} GeV.

The fact that the CMB fluctuation spec-

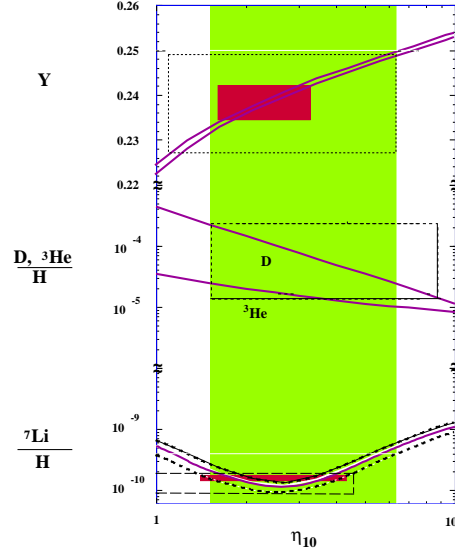


Figure 2. There is good concordance between the observed abundances of light elements and calculations of Big-Bang nucleosynthesis [6].

trum is largest for partial waves $\ell \sim 200$, as seen in Fig. 3 [7], suggests that the total energy density of the Universe is close to the critical density: $\Omega_{tot} \sim 1$. On the other hand, the Big-Bang nucleosynthesis calculations shown in Fig. 2 indicate that the density of baryons in the Universe today is far less than the critical density: $\Omega_B \equiv \rho_B/\rho_{crit} \sim$ few %, a range supported by observations of the smaller-scale peaks in the CMB fluctuations shown in Fig. 3. What form does the missing energy take?

Observations of large-scale structure suggest that the total matter density $\Omega_m \sim 0.3$, a value supported by a combination [8] of data on CMB fluctuations and high-redshift supernovae [9]. Most of this Ω_m is thought to be dark non-baryonic matter. What is the nature of this dark matter?

It certainly includes neutrinos, which are now thought to have non-zero masses [2,10], but these are probably insufficient to explain most of the dark matter. In any case, people who model the formation of large-scale structures would prefer more massive ‘cold’ dark matter particles that would have been non-relativistic when these structures began to grow. In addition to this cold dark matter,

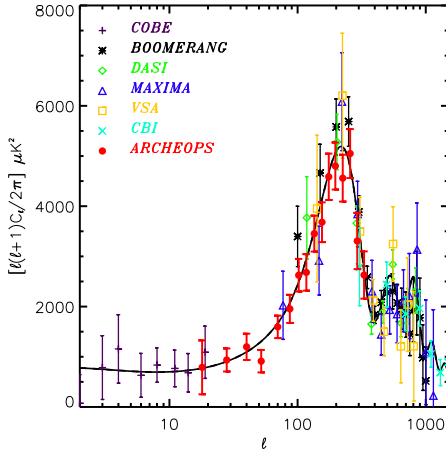


Figure 3. A compilation of data on fluctuations in the cosmic microwave background radiation [7].

the CMB and other data apparently require about $2/3$ of the critical density to be in the form of ‘dark energy’ in the vacuum [9,8], but I do not discuss the latter further in this talk. Instead, I concentrate on the dark-matter particles that might have signatures among high-energy cosmic rays.

3. Astrophysical Neutrinos

Let us first consider generic features of the density of relic neutrinos or similar neutral weakly-interacting particles. If neutrinos weigh less than ~ 1 MeV, their cosmological relic number density n_ν was fixed when $T \sim 1$ MeV and is essentially independent of their mass, hence their relic density $\rho_\nu = m_\nu n_\nu$ increases linearly with mass, rising above the critical density when $m_\nu \sim 30$ eV. The neutrino mass density would be excessive for masses up to ~ 3 GeV, where a Boltzmann factor suppresses the ν number density sufficiently to push Ω_ν back below unity. The ‘neutrino’ density would be most suppressed for $m_\nu \sim m_Z/2$, when ‘relic’ annihilation is most efficient. For larger ‘neutrino’ masses, the annihilation rate typically falls and the relic density (which is fixed when $T \sim m_\nu/25$) correspondingly rises, reaching the critical density for some ‘neutrino’ mass ~ 1 TeV.

Thus, there are three mass ranges where such a ‘neutrino’ might have a relic density of interest for astrophysics and cosmology: when $m_\nu \sim 10$ eV, ~ 3 GeV or ~ 100 GeV to 1 TeV. In the first of these windows, the neutrino would constitute hot dark matter, in the latter two it would be cold dark matter. The middle option is excluded by a combination of experiments at LEP and direct dark-matter searches, and the third option is that exercised by the lightest supersymmetric particle [11], as we discuss later.

Observations of large-scale structures in the Universe favour the predominance of cold dark matter, as already mentioned, and can be used to set an upper limit on the sum of light neutrino masses [12]:

$$\Sigma_i m_{\nu_i} < 3 \text{ eV}, \quad (1)$$

as seen in Fig. 4. The neutrino oscillation experiments force all three neutrino flavours to be essentially degenerate compared to (1), implying that $m_{\nu_i} < 1$ eV for each species. This is stronger than the upper limit $m_{\nu_e} < 2.5$ eV coming from the end-point of Tritium β decay [13], and future observations of large-scale structure should improve the sensitivity to $m_\nu \sim 0.3$ eV.

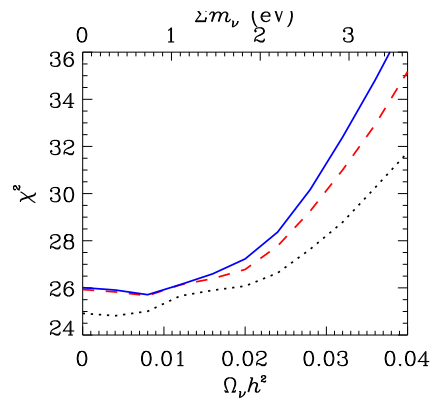


Figure 4. Cosmological upper limits on the neutrino mass [12], based on various combinations of data on the cosmic microwave background radiation and large-scale structures in the Universe.

Astrophysical sources [14] have provided

us with the first confirmed evidence for neutrino oscillations and (presumably) neutrino masses. The first astronomical image obtained with neutrinos was that of the Sun, via neutrino-electron scattering. Recently, comparative measurements of charged-current and neutral-current reactions by SNO [10] have established beyond any doubt that solar ν_e oscillate into some combination of ν_μ and ν_τ , most probably with a relatively large mass-squared difference $\Delta m^2 \sim 6 \times 10^{-5} \text{ eV}^2$ and relatively large, but not maximal, mixing $\sin^2 2\theta \sim 0.8$ (the LMA solution), as seen in Fig. 5 [10].

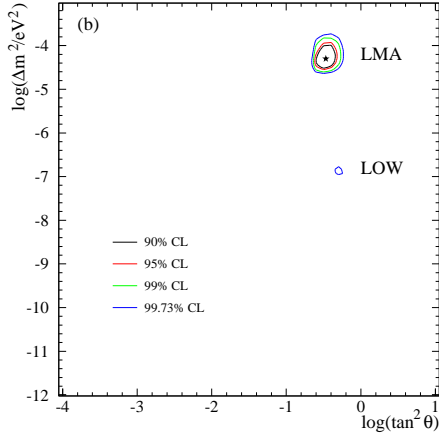


Figure 5. A global fit to solar neutrino data, following the SNO measurements of the total neutral-current reaction rate, the energy spectrum and the day-night asymmetry, favours large mixing and $\Delta m^2 \sim 6 \times 10^{-5} \text{ eV}^2$ [10].

As you know, atmospheric neutrinos are produced by cosmic rays with energies mainly in the range $\sim 1 - 10 \text{ GeV}$. For some time now, it has been established that ν_μ also oscillate [2], probably mainly into ν_τ with $\Delta m^2 \sim 2.5 \times 10^{-3} \text{ eV}^2$ and near-maximal mixing $\sin^2 2\theta \sim 1$, as seen in Fig. 6. The available data on the primary cosmic-ray spectrum and particle production at accelerators enable the atmospheric neutrino flux to be calculated quite reliably, and further improvements will be possible using the data presented here from the AMS [15] and L3+C [16] Collaborations.

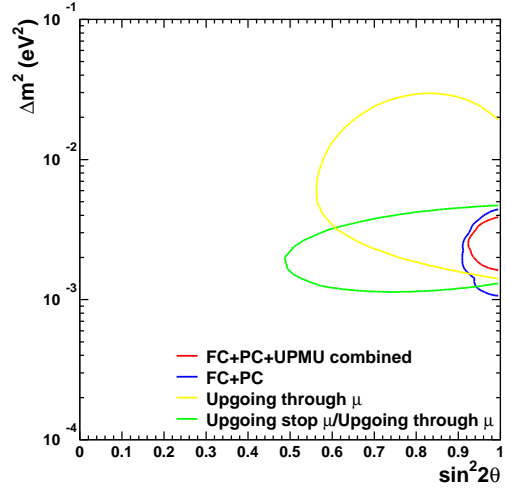


Figure 6. A fit to the Super-Kamiokande data on atmospheric neutrinos [2] indicates near-maximal $\nu_\mu - \nu_\tau$ mixing with $\Delta m^2 \sim 2.5 \times 10^{-3} \text{ eV}^2$.

Long-baseline neutrino oscillation experiments are underway to refine and extend these astrophysical neutrino oscillation results. The K2K experiment already provides some confirmation of atmospheric ν_μ oscillations, as seen in Fig. 7 [17], the KamLAND experiment is expected soon to test definitively the LMA solution for solar neutrinos [18], the MINOS experiment will look explicitly for the oscillatory pattern and have improved sensitivity to $\nu_\mu \rightarrow \nu_e$ oscillations [19], and the OPERA and ICARUS experiments should be able to observe the τ production expected following $\nu_\mu \rightarrow \nu_\tau$ oscillations [20].

4. Supersymmetry

As already mentioned, cosmic rays in the range from 100 GeV to 1 TeV may be the best place to look for supersymmetry: why? The primary theoretical motivation for expecting supersymmetry to appear in this energy range is provided by the hierarchy problem [21]: why is the electroweak scale m_W so much less than the Planck scale $m_P \sim 10^{19} \text{ GeV}$, which is the only candidate we have for a fundamental mass scale in physics? Equivalently, why is $G_F \sim 1/m_W^2 \ll G_N = 1/m_P^2$?

You might just say, why not choose the value of m_W and forget about the problem?

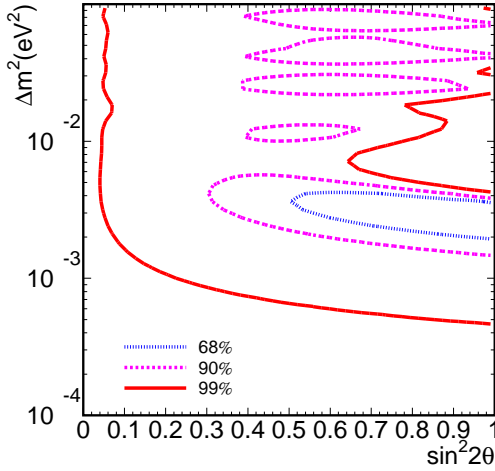


Figure 7. The region of Δm^2 and the mixing angle favoured by preliminary data from the K2K long-baseline experiment is highly consistent with the Super-Kamiokande data shown in Fig. 6 [17].

Life is not as simple as that, because quantum effects in the Standard Model make very large corrections to the electroweak scale:

$$\delta m_W^2 \sim \mathcal{O}\left(\frac{\alpha}{\pi}\right)\Lambda^2, \quad (2)$$

where Λ is a cutoff representing the scale at which the Standard Model must be modified by introducing new physics. A mechanism for cutting the divergence (2) off in a natural way is provided by supersymmetry, which exploits the opposite signs in the quadratically divergent fermionic and bosonic corrections to the electroweak scale:

$$\delta m_W^2 \sim \mathcal{O}\left(\frac{\alpha}{\pi}\right)|m_B^2 - m_F^2|, \quad (3)$$

which $\sim m_W^2$ if $|m_B^2 - m_F^2| \sim 1 \text{ TeV}^2$. This argument therefore leads one to expect supersymmetric partners of Standard Model particles to appear at or below the TeV scale [21].

This argument for low-energy supersymmetry is supported circumstantially by the possibility it offers for unification of the gauge couplings. Such grand unification does not occur in the absence of supersymmetry, but is quite possible if supersymmetric particles weigh about 1 TeV, as seen in Fig. 8 [22].

In many supersymmetric models, the lightest supersymmetric particle (LSP) χ is sta-

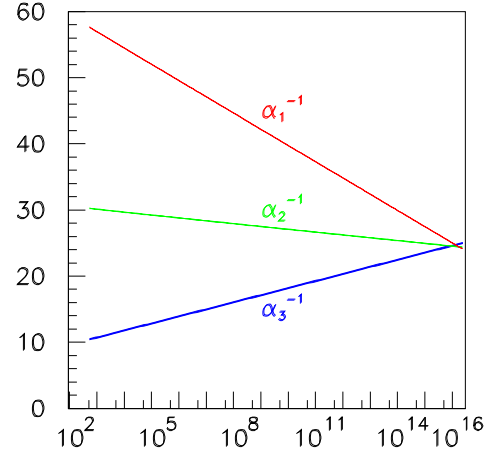


Figure 8. The measurements (vertical axis) of the gauge coupling strengths of the Standard Model at LEP and elsewhere can be evolved up to high energies (horizontal axis, in units of GeV) using renormalization-group equations incorporating supersymmetry. They are consistent with unification at a very high energy scale, but not with unification without supersymmetry [22].

ble, and a good candidate for cold dark matter [11], which provides a third general argument for the TeV mass scale. The relic energy density $\rho_\chi = m_\chi n_\chi$, where the relic number density

$$n_\chi \sim \frac{1}{\sigma_{ann}(\chi\chi \rightarrow \text{all})}, \quad (4)$$

where a typical annihilation cross section $\sigma_{ann} \sim 1/m_\chi^2$. Thus, the overall relic density increases with mass, and typically becomes too high when $m_\chi > 1 \text{ TeV}$.

However, the dark-matter annihilation rate may in exceptional circumstances be enhanced, reducing the supersymmetric relic density for a given mass, and thereby allowing larger relic masses. For example, if the LSP and the next-to-lightest supersymmetric particle \tilde{X} have similar masses, n_χ may be suppressed by coannihilation processes [23]: $\sigma(\chi\tilde{X} \rightarrow \text{all})$, which can be important if $m_{\tilde{X}} - m_\chi/m_\chi \sim 1/10$. This coannihilation

mechanism can provide an allowed ‘tail’ of parameter space extending out to larger m_χ , as seen in Fig. 9. Such a tail may also happen when rapid annihilation through a direct-channel pole is possible, for example if $m_\chi \sim m_{H,Z,\dots}/2$ [24].

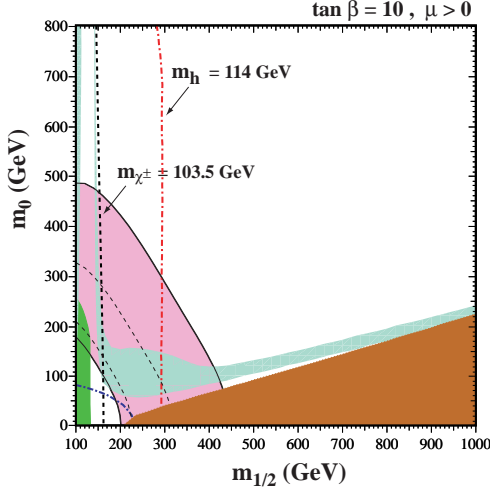


Figure 9. The parameter space of the MSSM projected onto the $(m_{1/2}, m_0)$ plane for $\tan\beta = 10$ and $\mu > 0$. The LEP lower limits on the Higgs, chargino and selectron masses are shown as (red) dot-dashed, (black) dashed and (blue) dash-dotted lines, respectively. The region at small $(m_{1/2}, m_0)$ excluded by $b \rightarrow s\gamma$ is shaded (green). The dark (red) shaded region is excluded because dark matter must be neutral, and the region where its relic density falls within the range preferred by cosmology has light (turquoise) shading. The region preferred by the BNL measurement of $g_\mu - 2$ and low-energy e^+e^- data is shaded (pink) [25].

The space of input supersymmetric fermion masses $m_{1/2}$ and boson masses m_0 is illustrated for one particular ratio $\tan\beta$ of the Higgs vacuum expectation values in the minimal supersymmetric extension of the Standard Model (MSSM) in Fig. 9 [25]. We see at large values of the ratio $m_{1/2}/m_0$ a region excluded because there the relic particle would be charged, a possibility excluded by astrophysics. At small $m_{1/2}$ and/or m_0 we see ex-

perimental exclusions from the absences of the supersymmetric partners of the electron \tilde{e} and of the W/H^\pm , and also of the Higgs boson H . A dark (green) shaded region is excluded by measurements of $b \rightarrow s\gamma$ decay, and a lighter (pink) shading shows regions favoured by the recent measurement of the anomalous magnetic moment of the muon [26].

Finally, the lightest (turquoise) shading in Fig. 9 picks out the region where the relic LSP density lies within the range favoured by cosmology: $0.1 < \Omega_\chi h^2 < 0.3$. We see that much of this region is disfavoured by the accelerator constraints, particularly the LEP Higgs limit $m_H > 114$ GeV [27].

A set of ‘benchmark’ supersymmetric scenarios was recently proposed [28], that respect all the experimental and cosmological constraints on the minimal supersymmetric extension of the Standard Model (MSSM). As shown in Fig. 10, they indicate the range of options, rather than sample the parameter space in a ‘fair’ manner. The LHC has great possibilities for detecting supersymmetry, principally via events with missing energy and other signatures such as high-energy leptons and/or jets. These prospects for discovering supersymmetry may be compared with those for detecting astrophysical supersymmetric dark matter.

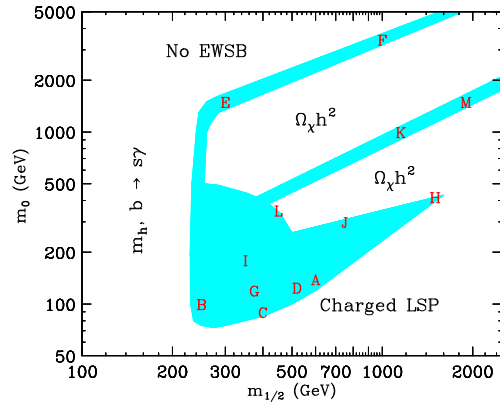


Figure 10. Sketch of the distribution of proposed CMSSM benchmark points in the $(m_{1/2}, m_0)$ plane [28]. These points were chosen as illustrations of the range of possibilities in the CMSSM, rather than as a ‘fair’ sample of its parameter space.

5. Search for Supersymmetric Dark Matter

Searches among cosmic rays with energies up to about 1 TeV provide several promising signatures for supersymmetric dark matter particles, that may enable this community to ‘scoop’ the LHC [29].

One possibility is to look for energetic *gamma rays* that may be emitted by LSP annihilations in the core of the Milky Way. The benchmark models indicate that these might have typical energies ~ 10 GeV, and detectors such as GLAST with a threshold as low as ~ 1 GeV might have a better chance, as seen in Fig. 11 [30]. The prospects for these searches depend on the degree to which the dark-matter particle density may be enhanced in the core of the Milky Way, which is uncertain by orders of magnitude. In Fig. 11, a middle-of-the-road enhancement by a factor 200 has been assumed.

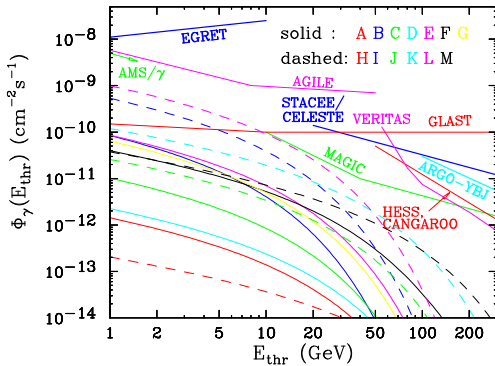


Figure 11. Observations of γ rays from the galactic centre by GLAST and ground-based experiments may be able to test certain supersymmetric benchmark scenarios [30].

Another possibility is to look for *positrons* emitted by LSP annihilations in the halo of the Milky Way. In this case, the benchmark models indicate that energies ~ 100 GeV might be the most interesting, though the signal may be less promising than in the γ case, as seen in Fig. 12 [30].

One of the most promising signatures is *energetic muons* produced in the Earth by energetic neutrinos emitted by LSP annihilations

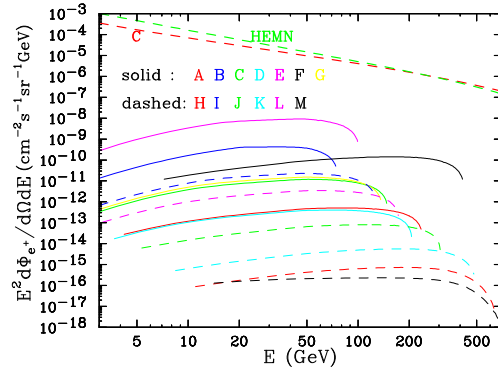


Figure 12. Comparison between the cosmic-ray positron background and the fluxes from the annihilations of relic particles, calculated [30] in supersymmetric benchmark scenarios.

in the centre of the Sun or Earth. In this case, as seen in Fig. 13, all energies up to ~ 1 TeV might be important. According to our calculations [30], the prospects for detecting relic annihilations in the core of the Sun appear more promising than those in the centre of the Earth. Some upper limits on the energetic solar muon flux have already been produced, most recently by the AMANDA Collaboration [31], which already begin to exclude some more extreme supersymmetric models.

The most convincing evidence for supersymmetric dark matter might eventually come from direct searches for the *scattering of relic particles* on nuclei in the laboratory [32]. Here the best chances seem to be offered by spin-independent scattering on relatively heavy nuclei. There has been a claim by the DAMA Collaboration [33] to have observed an annual modulation effect due to the scattering of dark matter particles, but this interpretation of their data has been largely excluded by the CDMS [34], EDELWEISS [35] and UKDMC experiments. In any case, reproducing the DAMA data would have required a scattering cross section much larger than predicted in the simple supersymmetric models studied in [30] and [36]. As illustrated in Fig. 14, future large cryogenic detectors, such as that proposed by the Heidelberg group, would good chances in many supersymmetric scenarios.

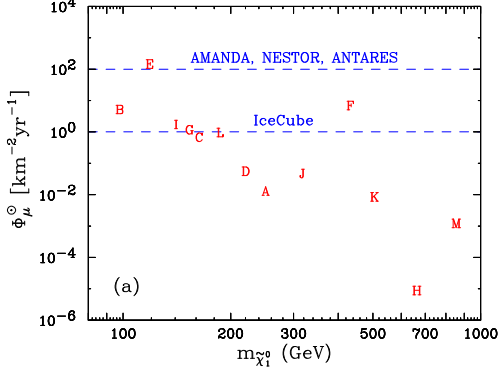


Figure 13. Searches in IceCube and other km² detectors for energetic muons originating from the interactions of high-energy neutrinos produced by the annihilations of supersymmetric relic particles captured inside the Sun may probe some supersymmetric benchmark scenarios [31].

6. Space-Time Foam

We know that space-time is essentially flat at large scales, but quantum gravitational effects are expected to cause large fluctuations on small scales in length and time:

$$\Delta E, \Delta \chi = \mathcal{O}(1) \text{ in } \Delta x, \Delta t = \mathcal{O}(1), \quad (5)$$

where the energy E , distance x and time t are all measured in Planck units $\sim 10^{19}$ GeV, $\sim 10^{-33}$ cm and $\sim 10^{-43}$ s, respectively, and χ is a generic dimensionless measure of topology. Are there any observable consequences of such quantum gravitational effects?

One suggestion has been that information might be lost across microscopic event horizons associated with such topological fluctuations, causing an apparent modification of microscopic quantum mechanics [37,38,39]. Another has been that the gravitational recoil of the vacuum as an energetic particle passes by might modify special relativity, in such a way that the particle's velocity might be reduced [40,41]:

$$c(E) = c \times \left(1 - \frac{E}{M} + \dots\right), \quad (6)$$

where M is a quantum-gravity mass scale that might $\sim m_P \sim 10^{19}$ GeV.

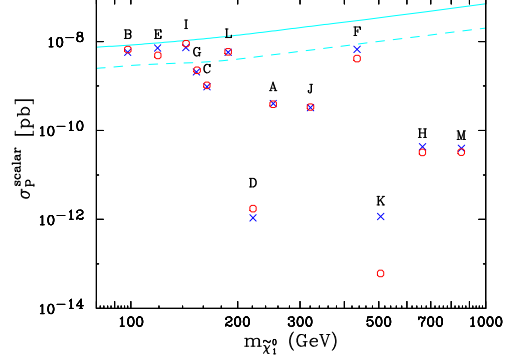


Figure 14. Direct searches for the scattering of supersymmetric relic particles in underground detectors may probe some supersymmetric benchmark scenarios [30].

The best probes of the possibility (6) may be provided by astrophysical sources of γ rays: they have large distances D and hence light propagation times $t = D/c$, and hence their light pulses may exhibit time delays

$$\Delta t \sim -\frac{D}{c^2}(c(E) - c). \quad (7)$$

Distant high-energy sources with short characteristic time scales δt have the best sensitivity to the quantum-gravity scale [41]:

$$M \sim \frac{E \cdot D}{\delta t}. \quad (8)$$

From this point of view, interesting astrophysical sources include pulsars (relatively short distances, but short time scales), AGNs (moderate redshifts z and relatively large time scales, but high energies) and GRBs ($z \sim 1$, $\delta t \sim 10^{-2}$ s). There are confirmed observations of GRBs only at relatively low energies, but there have been reports of GeV or even TeV [3] photons emitted by GRBs.

Some time ago, we published an analysis of all the GRBs whose redshifts had then been measured, using data from the BATSE and OSSE instruments on the Compton Gamma-Ray Observatory (CGRO), finding no significant correlation of time-lag with z , and inferring that $M \gtrsim 10^{15}$ GeV [42]. More recently, we have been making an improved analysis, benefiting from the measurements of more GRB redshifts, and using TTE data

from BATSE, which has a finer time resolution, and making a wavelet analysis, whose result is shown in Fig. 15. This time, we find $M \gtrsim 7.9 \times 10^{15}$ GeV [43]. In the future, GLAST should be able to improve significantly on this sensitivity [44].

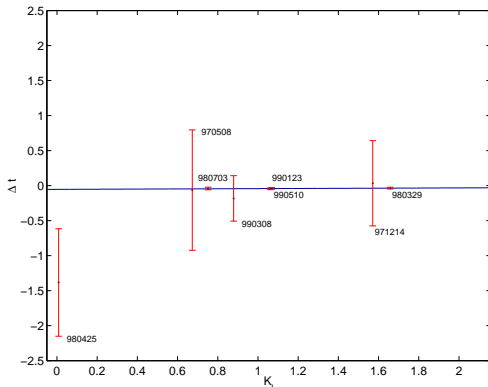


Figure 15. Search for a correlation with distance $\propto K_l$ of the time-lags Δt between structures in GRB emissions at different energies, as observed by the BATSE and OSSE instruments on the CGRO [43].

7. High-Energy Cosmic Rays and the LHC

Colliding pairs of protons with 14 TeV each, the LHC will be equivalent to a beam of particles with energies 10^{17} GeV striking a fixed target. The general-purpose detectors, ATLAS [45] and CMS [46], are designed to see ‘everything’ emitted with a centre-of-mass rapidity $|\eta| \lesssim 3$. The LHCb experiment [47] will also be able to measure some diffractive physics. The LHC will also be able to collide beams of heavy ions with energies ~ 5 TeV per nucleon, with the ALICE experiment [48] as principal user, and could in principle also collide protons or deuterons with heavy ions. Also planned is the TOTEM experiment [49] to measure the total and elastic pp cross sections, as well as some diffractive inelastic events. This experiment will have some capabilities to measure particles with $|\eta| \lesssim 3$ or 5, and the LHC physics community would like to hear from the cosmic-ray community what

its needs are [50]. This is the subject of a special workshop at this meeting: we hope that the LHC can contribute to refining models of ultra-high-energy cosmic rays. We should like to know what particles the cosmic-ray community would like to see measured in what rapidity range.

8. Ultra-High-Energy Cosmic Rays

As you know, extended-air-shower (EAS) experiments [51] have reported an apparent excess of events beyond the GZK cutoff, but this is not confirmed by HiRes [52], the largest fluorescence detector, as seen in Fig. 16. At issue are the absolute and relative energy calibrations of the EAS and fluorescence techniques. The former depends on the models that we hope the LHC will help refine, and the latter rely on normalizations of fluorescence lines around 390 nm. A recent experiment seems to find a discrepancy with previous measurements in this region, and the apparent conflict should be clarified [53].

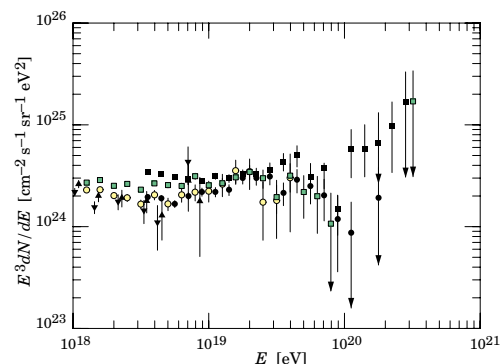


Figure 16. Compilation of data on ultra-high-energy cosmic rays [13]. AGASA and other experiments have reported some events beyond the GZK cutoff [51], but the HiRes experiment [52] (lighter symbols) reports no significant excess.

There are two main classes of models for ultra-high-energy cosmic rays (UHECR): ‘bottom-up’ and ‘top-down’. The former postulate acceleration by astrophysical sources,

which should have a minimum size R :

$$R \sim \frac{100}{Z} \left(\frac{E}{10^{20} \text{ eV}} \right) \left(\frac{\mu\text{G}}{B} \right), \quad (9)$$

where Z is the atomic number, E is the energy and B is the magnetic field bending the UHECR. Alternatively, the maximum energy attainable in any given source is

$$E \sim 10^{18} Z \left(\frac{R}{\text{Kpc}} \right) \left(\frac{B}{\mu\text{G}} \right) \text{ eV}. \quad (10)$$

Popular candidate sources include GRBs and AGNs, with neutron stars and colliding galaxies also proposed.

The alternative class of ‘top-down’ models postulates the production of UHECR by GUT-scale physics, such as topological defects or the decays of metastable superheavy relic particles [4] - which have some chances of being produced with interesting cosmological relic densities [54]. These models predict some anisotropy if the particles have a typical halo distribution [55], and could also exhibit clustering if the halo is lumpy [56]. A characteristic of ‘top-down’ models is that they predict large numbers of photons among the UHECR, and possibly even supersymmetric particles [57]!

Other suggestions for UHECR include the collisions of ultra-high-energy neutrinos with non-relativistic massive neutrinos to produce Z bosons [58,59]. It has also been suggested [5] that the type of modification of Lorentz kinematics mentioned earlier might also help distant sources evade the GZK cut-off.

There will be much discussion of these ideas during this meeting. We are all glad that the Auger experiment in Argentina is progressing well [60]. Its high statistics and combination of the EAS and fluorescence techniques should pin down the existence of UHECR and discriminate between rival models. In the longer run, the EUSO project [61] would be able to provide even higher statistics.

9. Conclusions

This talk has provided only a brief review of the interfaces between high-energy physics, astrophysics and cosmology. As we have seen, high-energy cosmic-ray physics may provide much useful information to particle physicists, for example concerning neutrinos and dark

matter, and possibly even quantum gravity. Likewise, accelerator experiments can provide useful input for cosmic-ray experiments, for example by testing, calibrating and validating simulation codes.

During this talk, we have discussed both localized astrophysical sources of high-energy particles and global sources provided by the very early Universe. Although lower-energy cosmic rays are believed to originate from local sources within our own galaxy, the origin of the highest-energy cosmic rays is still unknown. Both astrophysical sources and cosmological origins are being actively proposed. Unravelling the origins of the UHECR will surely require an active dialogue between accelerator and cosmic-ray physicists.

REFERENCES

1. B. Wiebel-Sooth, Ph. D. Thesis, University of Wuppertal preprint WUB-DIS-98-9.
2. Y. Fukuda *et al.* [Super-Kamiokande Collaboration], Phys. Rev. Lett. **81** (1998) 1562 [arXiv:hep-ex/9807003].
3. R. Atkins *et al.* [Milagro Collaboration], arXiv:astro-ph/0001111.
4. J. R. Ellis, J. L. Lopez and D. V. Nanopoulos, Phys. Lett. B **247** (1990) 257; J. R. Ellis, G. B. Gelmini, J. L. Lopez, D. V. Nanopoulos and S. Sarkar, Nucl. Phys. B **373** (1992) 399; V. Berezhinsky, M. Kachelriess and A. Vilenkin, Phys. Rev. Lett. **79** (1997) 4302 [arXiv:astro-ph/9708217]; M. Birkel and S. Sarkar, Astropart. Phys. **9** (1998) 297 [arXiv:hep-ph/9804285].
5. L. Gonzalez-Mestres, arXiv:hep-th/0210141, and references therein; S. R. Coleman and S. L. Glashow, arXiv:hep-ph/9808446.
6. For a recent review, see: K. A. Olive, arXiv:astro-ph/0202486.
7. A. Benoit [Archeops Collaboration], arXiv:astro-ph/0210306 contains references to previous data.
8. N. A. Bahcall, J. P. Ostriker, S. Perlmutter and P. J. Steinhardt, Science **284** (1999) 1481 [arXiv:astro-ph/9906463].
9. A. G. Riess *et al.* [Supernova Search Team Collaboration], Astron. J. **116** (1998) 1009 [arXiv:astro-ph/9805201]; S. Perlmutter *et al.* [Supernova Cosmology

- Project Collaboration], *Astrophys. J.* **517** (1999) 565 [arXiv:astro-ph/9812133].
10. Q. R. Ahmad *et al.* [SNO Collaboration], *Phys. Rev. Lett.* **87** (2001) 071301 [arXiv:nucl-ex/0106015], *Phys. Rev. Lett.* **89** (2002) 011301 [arXiv:nucl-ex/0204008], *Phys. Rev. Lett.* **89** (2002) 011302 [arXiv:nucl-ex/0204009].
 11. J. R. Ellis, J. S. Hagelin, D. V. Nanopoulos, K. A. Olive and M. Srednicki, *Nucl. Phys. B* **238** (1984) 453.
 12. S. Hannestad, arXiv:astro-ph/0205223.
 13. K. Hagiwara *et al.* [Particle Data Group Collaboration], *Phys. Rev. D* **66** (2002) 010001.
 14. See the 2002 Nobel Prize citation: <http://www.nobel.se/physics/laureates/2002/>.
 15. M. Aguilar *et al.* [AMS Collaboration], *Phys. Rept.* **366** (2002) 331.
 16. O. Adriani *et al.*, *Nucl. Instrum. Meth. A* **488** (2002) 209.
 17. Y. Oyama, arXiv:hep-ex/0210030.
 18. S. A. Dazeley [KamLAND Collaboration], arXiv:hep-ex/0205041.
 19. P. S. Miyagawa [MINOS Collaboration], *Prog. Part. Nucl. Phys.* **48** (2002) 111.
 20. D. Duchesneau [OPERA Collaboration], arXiv:hep-ex/0209082.
 21. L. Maiani, *Proceedings of the 1979 Gif-sur-Yvette Summer School On Particle Physics*, 1; G. 't Hooft, in *Recent Developments in Gauge Theories, Proceedings of the Nato Advanced Study Institute, Cargese, 1979*, eds. G. 't Hooft *et al.*, (Plenum Press, NY, 1980); E. Witten, *Phys. Lett. B* **105** (1981) 267.
 22. J. Ellis, S. Kelley and D. V. Nanopoulos, *Phys. Lett. B* **260** (1991) 131; U. Amaldi, W. de Boer and H. Furstenuau, *Phys. Lett. B* **260** (1991) 447; C. Giunti, C. W. Kim and U. W. Lee, *Mod. Phys. Lett. A* **6** (1991) 1745.
 23. J. R. Ellis, T. Falk and K. A. Olive, *Phys. Lett. B* **444** (1998) 367 [arXiv:hep-ph/9810360]; J. R. Ellis, T. Falk, K. A. Olive and M. Srednicki, *Astropart. Phys.* **13** (2000) 181 [Erratum-ibid. **15** (2001) 413] [arXiv:hep-ph/9905481]; and references therein.
 24. J. R. Ellis, T. Falk, G. Ganis, K. A. Olive and M. Srednicki, *Phys. Lett. B* **510** (2001) 236 [arXiv:hep-ph/0102098]; and references therein.
 25. J. Ellis, T. Falk, K. A. Olive and Y. Santoso, arXiv:hep-ph/0210205.
 26. G. W. Bennett *et al.* [Muon g-2 Collaboration], *Phys. Rev. Lett.* **89** (2002) 101804 [Erratum-ibid. **89** (2002) 129903] [arXiv:hep-ex/0208001].
 27. LEP Higgs Working Group for Higgs boson searches, OPAL Collaboration, ALEPH Collaboration, DELPHI Collaboration and L3 Collaboration, LHWG Note/2002-01, http://lephiggs.web.cern.ch/LEPHIGGS/papers/July2002_SM/index.html.
 28. M. Battaglia *et al.*, *Eur. Phys. J. C* **22** (2001) 535 [arXiv:hep-ph/0106204].
 29. For a review, see: L. Bergstrom, *Rept. Prog. Phys.* **63** (2000) 793 [arXiv:hep-ph/0002126].
 30. J. R. Ellis, J. L. Feng, A. Ferstl, K. T. Matchev and K. A. Olive, *Eur. Phys. J. C* **24** (2002) 311 [arXiv:astro-ph/0110225].
 31. J. Ahrens *et al.* [AMANDA Collaboration], arXiv:astro-ph/0208006.
 32. M. W. Goodman and E. Witten, *Phys. Rev. D* **31** (1985) 3059.
 33. R. Bernabei *et al.* [DAMA Collaboration], *Phys. Lett. B* **480** (2000) 23.
 34. D. Abrams *et al.* [CDMS Collaboration], arXiv:astro-ph/0203500.
 35. A. Benoit *et al.* [EDELWEISS Collaboration], *Phys. Lett. B* **513** (2001) 15 [arXiv:astro-ph/0106094].
 36. J. R. Ellis, A. Ferstl and K. A. Olive, *Phys. Lett. B* **532** (2002) 318 [arXiv:hep-ph/0111064].
 37. S. W. Hawking, *Commun. Math. Phys.* **87** (1982) 395.
 38. J. R. Ellis, J. S. Hagelin, D. V. Nanopoulos and M. Srednicki, *Nucl. Phys. B* **241** (1984) 381.
 39. J. R. Ellis, N. E. Mavromatos and D. V. Nanopoulos, *Phys. Lett. B* **293** (1992) 37 [arXiv:hep-th/9207103].
 40. G. Amelino-Camelia, J. R. Ellis, N. E. Mavromatos and D. V. Nanopoulos, *Int. J. Mod. Phys. A* **12** (1997) 607 [arXiv:hep-th/9605211].
 41. G. Amelino-Camelia, J. R. Ellis, N. E. Mavromatos, D. V. Nanopoulos and S. Sarkar, *Nature* **393** (1998) 763 [arXiv:astro-ph/9712103].
 42. J. R. Ellis, K. Farakos, N. E. Mavromatos, V. A. Mitsou and D. V. Nanopoulos, *As-*

- trophys. J. **535** (2000) 139 [arXiv:astro-ph/9907340].
43. J. R. Ellis, N. E. Mavromatos, D. V. Nanopoulos and A. S. Sakharov, arXiv:astro-ph/0210124.
 44. J. P. Norris, J. T. Bonnell, G. F. Marani and J. D. Scargle, arXiv:astro-ph/9912136.
 45. ATLAS Collaboration, <http://atlas.web.cern.ch/Atlas/Welcome.html>.
 46. CMS Collaboration, <http://cmsdoc.cern.ch/cms/outreach/html/index.shtml>.
 47. LHCb Collaboration, <http://lhcb.web.cern.ch/lhcb/>.
 48. ALICE Collaboration, <http://alice.web.cern.ch/Alice/>.
 49. TOTEM Collaboration, <http://totem.web.cern.ch/Totem/>.
 50. D. Heck, M. Risse and J. Knapp, arXiv:astro-ph/0210392.
 51. M. Takeda *et al.*, arXiv:astro-ph/0209422.
 52. T. Abu-Zayyad *et al.* [High Resolution Fly's Eye Collaboration], arXiv:astro-ph/0208243; arXiv:astro-ph/0208301.
 53. A. A. Watson, private communication.
 54. D. J. Chung, P. Crotty, E. W. Kolb and A. Riotto, Phys. Rev. D **64** (2001) 043503 [arXiv:hep-ph/0104100].
 55. N. W. Evans, F. Ferrer and S. Sarkar, Astropart. Phys. **17** (2002) 319 [arXiv:astro-ph/0103085].
 56. P. Blasi and R. K. Sheth, arXiv:astro-ph/0108288.
 57. C. Barbot, M. Drees, F. Halzen and D. Hooper, arXiv:hep-ph/0207133.
 58. T. J. Weiler, Astropart. Phys. **11** (1999) 303 [arXiv:hep-ph/9710431].
 59. Z. Fodor, S. D. Katz and A. Ringwald, arXiv:hep-ph/0210123.
 60. M. Dova, talk at this meeting; A. Letessier-Selvon, arXiv:astro-ph/0208526.
 61. L. Scarsi, *EUSO: Using high energy cosmic rays and neutrinos as messengers from the unknown universe*, in *Metepec 2000, Observing ultrahigh energy cosmic rays from space and earth*, p113.